Geochimica et Cosmochimica Acta Vol. 55, pp. 1121–1133

0016-7037/91/$3.00 + .00

The Estherville mesosiderite: U-Pb, Rb-Sr, and Sm-Nd isotopic study of a polymict breccia

M. BROUXEL* and M. TATSUMOTO
US Geological Survey, Branch of Isotope Geology, MS 963, PO Box 25046, Denver, CO 80225, USA

(*Received August* 27, 1990; *accepted in revised form January* 31, 1991)

Abstract—A systematic U-Pb, Sm-Nd, and Rb-Sr isotopic study shows that the Estherville mesosiderite was formed between 4.56 and 4.43 Ga. Observed isotopic heterogeneity is in agreement with multiple generations of meteoritic impacts described in other mesosiderites.

At least part of the Estherville silicate fraction was formed early in solar system history as indicated by the Pb-Pb (4555 ± 35 Ma), U-Pb (4560 ± 31 Ma), Rb-Sr (4542 ± 203 Ma), and Sm-Nd (4533 ± 94 Ma) ages. Mesosiderites therefore present not only petrological but also geochronological similarities with eucrites. The Pb isotopic composition of the metal phase plots on the same isochron as the silicates, indicating formation and subsequent mixing with silicates early in the history of the solar system. This is consistent with previous observations indicating that iron was reduced during the silicate-magmatic stage, most likely a consequence of mixing with metal.

In addition to these more-ancient portions of the Estherville breccia, other parts were formed later as suggested by the Pb-Pb (4422 ± 50 Ma) and U-Pb (4437 ± 11 Ma) ages observed in a second group of leaches and residues. This age is similar to some cumulate eucrite ages and may represent the formation of a second mesosiderite component.

The Sm-Nd and the Rb-Sr ages obtained on Estherville show large errors that may be a consequence of the mixing between the 4.56 and 4.43 Ga endmembers.

Estherville, like most mesosiderites, was affected by a major heating event around 3.5–3.7 Ga as shown by the Ar-Ar ages (BOGARD et al., 1990). This heating event partially disturbed the Rb-Sr isotopic system (Rb-Sr metamorphic ages range between 3.81 and 4.08 Ga).

INTRODUCTION

IN THE PAST FEW YEARS the petrology and geochemistry of mesosiderites have been intensely studied in order to better understand their origin(s) and age(s). However, they are still the matter of intense debates because of the very complicated nature of mesosiderites.

Mesosiderites contain approximately equal amounts of iron-nickel metal and silicates (PRIOR, 1920). The silicate fraction of mesosiderites is highly brecciated and contains a complex assemblage of minerals (orthopyroxene, plagioclase, and olivine) and lithic clasts (diogenites, cumulate eucrites, basaltic eucrites, and dunites; FLORAN, 1978). The silicates record magmatic (partial melting, differentiation) and metamorphic (recrystallization, impact melting, brecciation) events, and argue for an origin at, or near, a planetary surface (FLORAN, 1978; FLORAN et al., 1978; HEWINS, 1983). However, the mixing of silicates with metal appears to be hard to reconcile with a near-surface environment (DELANEY, 1983; GREENBERG and CHAPMAN, 1984).

Most of the models proposed for the origin of mesosiderites (mixing of silicates and iron either by interaction of a basaltic crust with the metal core, or by impact) require that the mesosiderites were formed early in the history of the solar system (BOGARD et al., 1990). However, until very recently, there was no such chronological evidence. Indeed, all ages obtained on mesosiderites were quite young compared to the 4.55 Ga age of Juvinas (ALLEGRÈ et al., 1975). Potassium-Argon and Argon-Argon ages of mesosiderites range between 3.23 and 4.25 Ga (MEGRUE, 1966; BEGEMANN et al., 1976; MURTHY et al., 1977, 1978; BOGARD et al., 1988, 1990). MURTHY et al. (1978) reported a 4.24 ± 0.03 Ga Rb-Sr age for Estherville while MITTLEFEHLDT et al. (1986a) showed young, likely disturbed, Rb-Sr model ages (≈3.6 Ga) for several other mesosiderites.

In the last two years, older internal isochrons were obtained for Morristown (4.47 ± 0.02 Ga by Sm-Nd; PRINZHOFER et al., 1989) and Estherville (4.56 ± 0.04 Ga and 4.57 ± 0.02 Ga by Pb-Pb and U-Pb; BROUXEL and TATSUMOTO, 1990) suggesting that at least some mesosiderites, or mesosiderite fractions, may have been formed early in solar system history. However, mesosiderites have likely been disturbed by a major heating event around 3.5–3.7 Ga, which is recorded by Ar-Ar ages (BOGARD et al., 1990). This event may have also affected some of the other isotopic systems. For a better understanding of this problem, a comparison of different chronological methods is required. In this paper, we examine the Estherville mesosiderite using U-Pb, Rb-Sr, and Sm-Nd isotopic systematics to help decipher the history of this polymict breccia. In a previous study of the U-Pb systematics of Estherville, we have suggested that different portions of the silicate fraction were formed at different times (Pb-Pb and U-Pb ages between 4.42 ± 0.05 Ga and 4.57 ± 0.02 Ga; BROUXEL and TATSUMOTO, 1990). Therefore, interpretation of the effects of metamorphism on the earlier igneous events is likely to be complicated by the polymict, rather than monomict, nature of the Estherville breccia (UNRUH et al., 1977).

* *Present address:* DUNE Travaux Spéciaux, Laboratoire d'Analyses et de Recherches, C.E.I., Campus Universitaire de la Doua, BP 2132, 69603 Villeurbanne Cedex, France.

SAMPLE PREPARATION

This study was conducted on a 13 g Estherville brecciated clast provided to us by V. R. Murthy from a slice kept at the University of Minnesota (the other portion is located now at the US National Museum). The sample was first washed for one minute using 1 N HCl in an ultrasonic bath and then rinsed repeatedly in distilled water. The sample was then crushed using a stainless steel mortar and divided into four sized fractions (<63 μm, 63–150 μm, 150–300 μm, >300 μm) using nylon cloth sieves. As much metal as possible was removed using a hand magnet. The different steps of the sample preparation are summarized in Fig. 1.

Twenty-one separates were obtained either by handpicking, or by using density and magnetic separation techniques. They were grouped into three sets analyzed for U-Pb (BROUXEL and TATSUMOTO, 1990), Rb-Sr, and Sm-Nd isotopes (set A), for U-Pb isotopes (set B), and for Rb-Sr and Sm-Nd isotopes (set C).

Set A (Nine Separates)

The finest grained fraction (<63 μm) was analyzed without further mineral separation as an approximation to the whole-rock (silicate fraction).

The 63–150 μm fraction was first leached twice, each time overnight (12 h), in weak acetic acid (1:4, 1× sub-boiling distilled) in order to remove the iron coating. A trial test showed that apatite (terrestrial) dissolved only slightly in 1:4 acetic acid (less than 4% in 24 h). This fraction was then separated into four density separates ($\rho < 2.58$, $2.58 < \rho < 2.95$, $2.95 < \rho < 3.3$, $\rho > 3.3$) using mixtures of methylene iodide and acetone. The two heaviest separates, still coated by iron, or containing "iron dandruff," were divided into two splits using a magnetic separator (quartz chute filled with 1× sub-boiling distilled ethanol). We used the density limits proposed by MURTHY et al. (1977) which were meant to separate orthopyroxene in the heaviest density separates, plagioclase in the 2.58–2.95 density separate, and the mesostasis (interstitial phases) into the lightest density separate.

Orthopyroxene and brecciated silicate fragments, apparently similar to the brecciated and angular polycrystalline fragments described by POWELL (1971), were handpicked from the coarse-grain fraction (>300 μm).

These nine separates were then stepwise leached, two times five minutes, in HBr (0.1 N and 0.5 N), HCl (2 N), and HF (1 N) + HNO_3 (2 N). All leaches and residues were analyzed.

In contrast to set A, separates of set B and C were leached as gently as possible in order to control the leaching effects on the U-Pb, Rb-Sr, and Sm-Nd isotopic systems.

Set B (Five Separates)

Five separates (plagioclase, orthopyroxene, iron, chromite, and troilite) were handpicked from the 150–300 μm fraction. Iron was

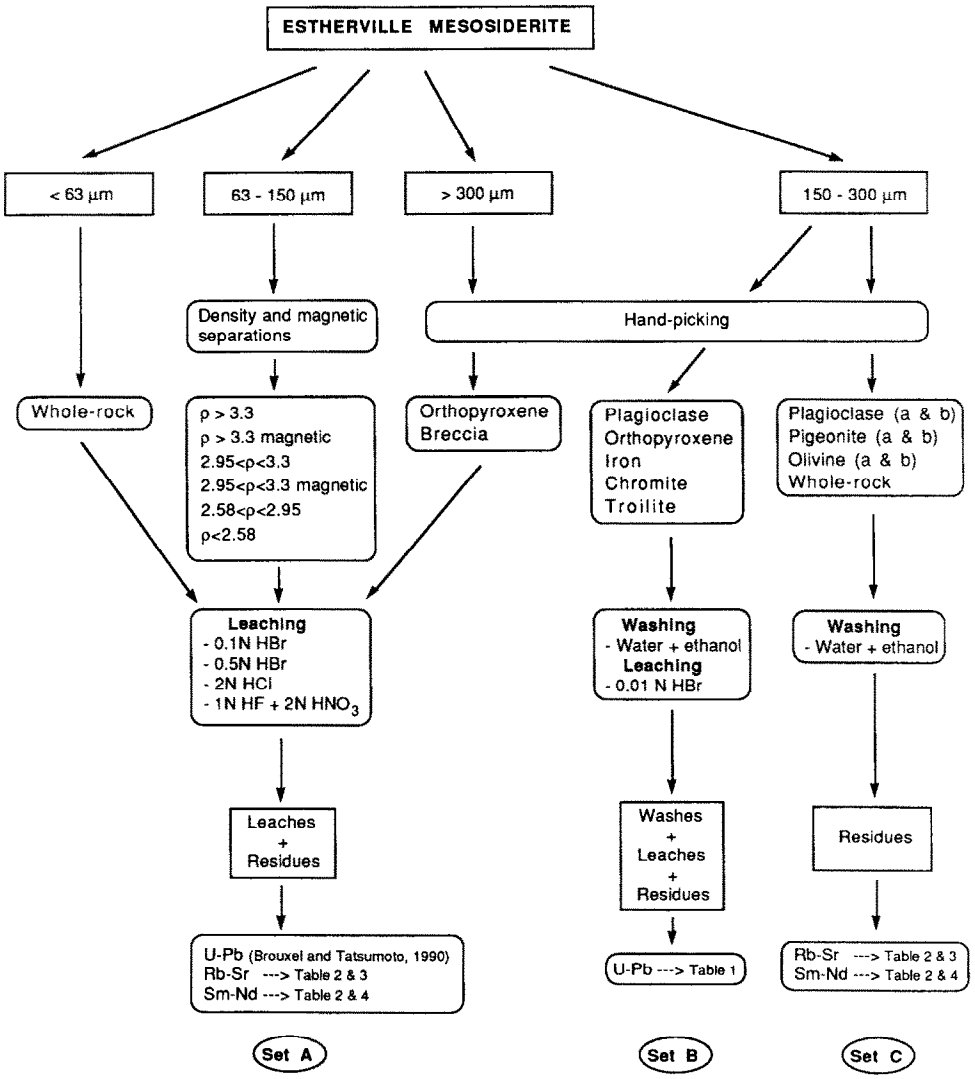

FIG. 1. Sample preparation procedure.

TABLE 1. U-Th-Pb analytical data for the Estherville mesosiderite (Set B : residues, water and ethanol washes, and dilute HBr leaches)

Sample	Weight (mg)	Pb † (ppb)	U † (ppb)	Th † (ppb)	$^{206}Pb/^{204}Pb$ †	$^{207}Pb/^{204}Pb$ †	$^{208}Pb/^{204}Pb$ †	$^{238}U/^{204}Pb$ †	$^{232}Th/^{238}U$ †	$^{206}Pb/^{238}U$ †*	$^{207}Pb/^{235}U$ †*	$^{207}Pb/^{206}Pb$ †*	$^{208}Pb/^{232}Th$ †*
Water and ethanol washes π													
Troilite	18.66	42.0	0.91	0.37	18.36 (0.16) ††	15.69 (0.24)	37.92 (0.25)	1.367 (5.1)	0.421 (10.5)	6.621 (5.2)	543.9 (5.4)	0.596 (1.1)	14.66 (10.6)
Chromite	3.21	92.0	1.64	1.68	18.56 (0.31)	15.67 (0.48)	37.92 (0.37)	1.127 (5.8)	1.057 (5.5)	8.211 (5.8)	658.0 (5.9)	0.581 (1.4)	7.088 (5.8)
Plagioclase	1.66	94.9	1.27	1.16	18.68 (0.53)	15.65 (0.64)	37.54 (0.60)	0.844 (7.7)	0.942 (10.6)	11.11 (7.7)	875.8 (7.8)	0.572 (1.1)	10.14 (10.2)
Orthopyroxene	8.97	69.3	0.25	0.19	18.06 (0.19)	15.60 (0.29)	37.65 (0.28)	0.225 (11.4)	0.766 (12.3)	38.81 (11.8)	3243 (11.5)	0.606 (1.2)	47.30 (12.8)
Very dilute HBr (0.01N) leaches													
Iron #	299.31	15.2	-	-	22.19 (0.12)	17.83 (0.17)	42.56 (0.21)	-	-	-	-	-	-
Troilite	18.66	167.2	0.97	1.46	18.51 (0.11)	15.83 (0.16)	38.14 (0.21)	0.367 (3.9)	1.557 (2.7)	25.07 (4.1)	2080 (4.4)	0.602 (0.97)	15.15 (3.0)
Chromite	3.21	349.7	1.14	3.48	18.66 (0.13)	15.72 (0.20)	38.22 (0.23)	0.207 (9.3)	3.152 (6.6)	45.16 (9.3)	3612 (9.3)	0.580 (1.1)	13.38 (6.7)
Plagioclase	1.66	191.4	2.46	6.48	18.89 (0.29)	15.92 (0.36)	38.26 (0.34)	0.821 (8.9)	2.728 (10.1)	11.67 (8.9)	944.8 (8.9)	0.587 (1.2)	3.922 (10.3)
Orthopyroxene	8.97	191.0	0.25	0.45	18.01 (0.12)	15.64 (0.18)	37.68 (0.22)	0.0827 (10.9)	1.852 (7.3)	105.2 (11.0)	8910 (11.0)	0.614 (1.0)	53.62 (7.4)
Residues													
Iron #	299.31	143.7	6.60	28.5	20.90 (0.10)	17.91 (0.16)	40.97 (0.20)	3.207 (0.36)	4.469 (0.19)	3.616 (1.0)	327.7 (1.4)	0.657 (0.68)	0.802 (1.0)
Troilite	18.63	42.2	0.936	2.19	18.84 (0.10)	16.26 (0.15)	38.82 (0.20)	1.438 (10.1)	2.421 (4.29)	6.630 (10.1)	572.2 (10.2)	0.626 (0.88)	2.683 (4.5)
Chromite	3.15	76.7	0.552	7.39	17.54 (0.57)	15.84 (0.65)	36.80 (0.82)	0.442 (8.8)	13.85 (6.2)	18.63 (9.0)	1730 (8.0)	0.674 (1.2)	1.196 (6.5)
Plagioclase	1.64	98.3	7.334	6.71	20.42 (0.42)	17.60 (0.60)	38.77 (0.57)	5.016 (19.3)	0.945 (19.3)	2.215 (17.7)	200.9 (16.7)	0.658 (0.92)	1.961 (19.2)
Orthopyroxene	8.86	14.8	0.606	1.26	19.56 (0.47)	17.04 (0.67)	38.88 (0.65)	2.708 (17.1)	2.149 (14.7)	3.785 (16.4)	343.6 (14.9)	0.658 (1.2)	1.617 (14.5)

† : Data corrected for mass fractionation and laboratory blank (Ludwig, 1985b; see text for details)
†† : 2 sigma errors (in percent)
π : Pb, U, and Th concentration of washes and leaches are shown against the starting weight
* : Data corrected for initial Pb (see text for details)
# : Iron was leached in HBr (0.1N) and dissolved in 6N HCl

leached two times five minutes with 0.1 N HBr and dissolved in 6 N HCl. All the other separates were washed with water and ethanol and then gently leached two times five minutes with very dilute HBr (0.01 N) in order to remove the contamination introduced during the sample preparation. All washes, leaches, and residues were analyzed.

Set C (Seven Separates)

Seven other separates (two plagioclase, two pigeonite, two olivine, and a whole rock) were also handpicked from the 150–300 μm fraction. These separates were washed with water and ethanol, and then analyzed for Rb-Sr and Sm-Nd.

ANALYTICAL PROCEDURES

The analytical procedures and mass spectrometric techniques for U-Pb, Rb-Sr, and Sm-Nd are similar to those reported in detail by NAKAMURA et al. (1976), TATSUMOTO et al. (1987), and PREMO et al. (1989).

The leaches and residues were spiked with one (^{233}U, ^{236}U, ^{232}Th, ^{205}Pb), two (^{87}Rb, ^{84}Sr and ^{149}Sm, ^{150}Nd) or three (U-Th-Pb, Rb-Sr, and Sm-Nd) mixed tracer solutions, dried down, and dissolved in concentrated HF + HNO_3.

Lead isotopic ratios were measured on single Re-filaments using the phosphoric acid–silica gel technique and corrected for a mass fractionation of 0.13 ± 0.05% per amu as determined by replicate analyses of an NBS SRM-982 Pb standard. The U and Th isotope ratios were measured using a triple Re (MARZ-grade) filament configuration, and U mass fractionation was corrected using ^{233}U/^{236}U spike ratios. All isotopic measurements were performed on an NBS-type two-stage mass spectrometer using an ion pulse counter at the end of the second stage. The analyses were corrected for laboratory U, Th, and Pb contamination (blank Pb had an isotopic composition of ^{206}Pb/^{204}Pb = 18.66 ± 0.15, ^{207}Pb/^{204}Pb = 15.57 ± 0.20, and ^{208}Pb/^{204}Pb = 38.52 ± 0.25) and for initial Pb using the Cañon Diablo Troilite primordial Pb isotopic composition of TATSUMOTO et al. (1973). A blank correction of 50 to 100 pg for Pb and 2 pg for U and Th were applied. Thorium and uranium decay constants used in this paper are, respectively, from LEROUX and GLENDENIN (1963) and JAFFEY et al. (1971).

Strontium and neodymium isotopic compositions were measured on a VG Micromass 54R mass spectrometer following the procedure described by LUDWIG (1985a). Strontium isotopic compositions were reduced from the spiked runs and were normalized to ^{86}Sr/^{88}Sr = 0.1194. Strontium was measured on a single W-filament using a Ta + H_3PO_4 activator (BIRCK, 1986). Measured values for NBS SRM-987 were ^{87}Sr/^{86}Sr = 0.710276 ± 15. Our Sr isotopic values were not corrected for interlaboratory bias. Neodymium was measured as NdO^+ using an oxygen leak. The oxygen isotopic composition of our reservoir was determined by running ^{150}Nd spike (^{150}Nd^{18}O/^{150}Nd^{16}O and ^{150}Nd^{17}O/^{150}Nd^{16}O). The Nd isotopic compositions were reduced from the spiked runs normalizing ^{146}Nd/^{144}Nd = 0.7219 (^{146}Nd^{16}O/^{144}Nd^{16}O = ^{162}NdO/^{160}NdO = 0.72226) following the method of WASSERBURG et al. (1981). The mean value of the La Jolla standard was ^{143}Nd/^{144}Nd = 0.511892 ± 10; therefore, our values were corrected to ^{143}Nd/^{144}Nd = 0.511860 (LUGMAIR and CARLSON, 1978; UNRUH et al., 1984). Total blanks were less than 0.05 ng for Rb and Sm, less than 0.1 ng for Nd, and less than 0.2 ng for Sr. The decay constants for ^{87}Rb and ^{147}Sm used in this paper are $\lambda = 1.42 \times 10^{-11}$ a^{-1} and 6.54×10^{-12} a^{-1}, respectively.

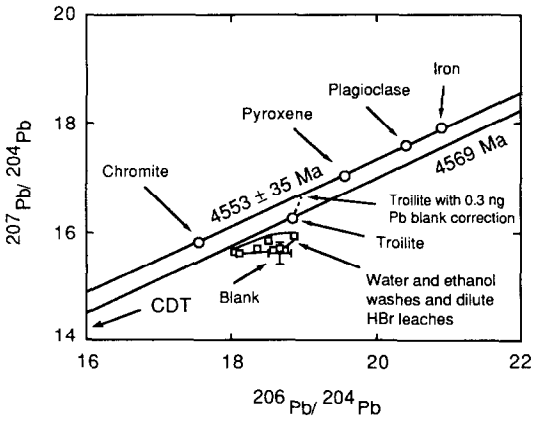

FIG. 2. ^{207}Pb/^{204}Pb vs. ^{206}Pb/^{204}Pb diagram of all the data of set B (washes, leaches, and residues). All ages were determined using the algorithms of LUDWIG (1980, 1985c), which use the regression approach of YORK (1969). Uncertainties are reported at the 95% confidence level.

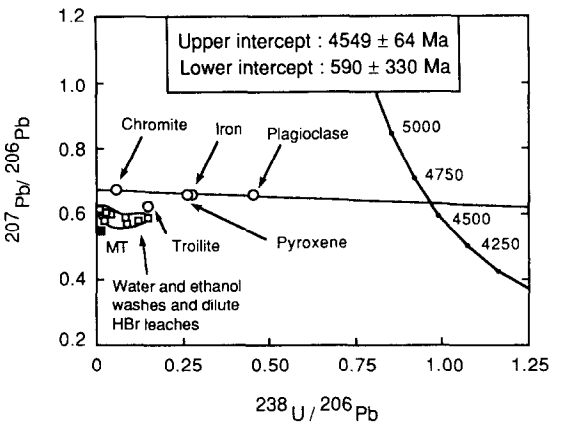

FIG. 3. ^{207}Pb/^{206}Pb vs. ^{238}U/^{206}Pb modified concordia diagram after TERA and WASSERBURG (1972) for all the data of set B (washes, leaches, and residues). MT = Modern Terrestrial Pb. The data were corrected for laboratory U, Th, and Pb contamination and for initial Pb using the Cañyon Diablo Troilite primordial Pb isotopic composition of TATSUMOTO et al. (1973).

RESULTS

All the Pb isotopic data of set A (50 analyses) plot on a 4228 ± 85 Ma Pb-Pb isochron, which has been interpreted as a two or more component mixing-line (the U-Pb data of set A were previously reported; BROUXEL and TATSUMOTO, 1990). These data were divided into four different groups based on their U-Pb isotopic compositions. Analyses of group 1, characterized by ^{207}Pb/^{206}Pb initial ratios $\approx$ 0.65, define, in the modified concordia diagram of TERA and WASSERBURG (1972), an almost horizontal chord intersecting concordia at 4571 ± 18 Ma and 144 ± 110 Ma. The U-Pb upper-intercept age is in agreement with the Pb-Pb age obtained when plotting these points in a ^{206}Pb/^{204}Pb vs. ^{207}Pb/^{204}Pb diagram (4556 ± 35 Ma). Analyses of group 2, characterized by ^{207}Pb/^{206}Pb initial ratios $\approx$ 0.58, also define an almost horizontal chord intersecting concordia at 4437 ± 11 Ma and −40 ± 56 Ma. Again, the U-Pb upper-intercept age is in agreement with the Pb-Pb age obtained when plotting these points on a ^{206}Pb/^{204}Pb vs. ^{207}Pb/^{204}Pb diagram (4422 ± 50 Ma). Data from group 3, characterized by ^{207}Pb/^{206}Pb initial ratios ranging between 0.67 and 0.85, and from group 4, characterized by ^{207}Pb/^{206}Pb initial ratios ranging between 0.7 and 1.0, cannot be strictly differentiated on the basis of their U-Pb data. They have likely been disturbed by our leaching procedure (variable ^{238}U/^{206}Pb isotopic ratios at constant ^{207}Pb/^{206}Pb initial isotopic ratios) and give conflicting

Table 2 : Rb-Sr and Sm-Nd concentrations of the analyzed leaches and residues of the Estherville mesosiderite

	Starting Weight (mg)	Residue (mg)	HBr (0.1N) leaches Sr ppm	Sr (ng)	Rb ppm	HCl (2N) leaches Sr ppm	Sr (ng)	Rb ppm	HF(1N)+HNO3(2N) leaches Sr ppm	Sr (ng)	Rb ppm	Residues Sr ppm	Sr (ng)	Rb ppm
Set A : Leached samples														
ρ > 3.3	96.06	70.36	0.073	(7)	0.0005	0.154	(15)	0.0001	1.91	(184)	0.0030	5.53	(389)	0.042
ρ > 3.3 magn.	94.51	88.09	0.121	(11)	0.0004	0.305	(29)	0.0002	2.43	(230)	0.0027	2.27	(200)	0.021
2.95<ρ<3.3	96.51	89.21	0.204	(20)	0.0014	0.574	(55)	0.0012	5.08	(490)	0.0056	4.37	(390)	0.046
2.95<ρ<3.3 magn.	95.27	66.00	0.256	(24)	0.0001	1.492	(142)	0.0027	7.25	(690)	0.0068	8.25	(545)	0.080
2.58<ρ<2.95	95.36	75.46	0.756	(72)	0.0021	0.683	(65)	0.0014	13.49	(1286)	0.0113	61.80	(4663)	0.252
ρ < 2.58	34.77	25.15	0.310	(11)	0.0029	0.911	(32)	0.0041	22.74	(791)	0.0375	80.96	(2036)	0.690
Opx	68.71	65.39	0.030	(2)	0.0005	0.106	(7)	0.0001	1.04	(72)	0.0019	1.20	(78)	0.022
Breccia	34.10	28.72	0.204	(7)	0.0027	0.172	(6)	0.0007	5.98	(204)	0.0092	19.82	(569)	0.304
Whole Rock	100.01	78.09	0.886	(89)	0.0024	1.577	(158)	0.0018	14.70	(1470)	0.0171	7.35	(574)	0.097
Set C : Unleached samples														
Plagioclase (a)	40.74											58.20	(2371)	0.215
Plagioclase (b)	42.69											65.47	(2795)	0.297
Pigeonite (a)	57.07											2.31	(132)	0.013
Pigeonite (b)	21.68											6.47	(140)	0.035
Whole Rock	35.16											6.96	(245)	0.034

	Starting Weight (mg)	Residue (mg)	HBr (0.1N) leaches Nd ppm	Nd (ng)	Sm ppm	HCl (2N) leaches Nd ppm	Nd (ng)	Sm ppm	HF(1N)+HNO3(2N) leaches Nd ppm	Nd (ng)	Sm ppm	Residues Nd ppm	Nd (ng)	Sm ppm
Set A : Leached samples														
ρ > 3.3	96.06	70.36	0.011	(1.1)	0.0035	0.008	(0.8)	0.0029	0.007	(0.7)	0.0015	0.096	(6.8)	0.0363
ρ > 3.3 magn.	94.51	88.09	0.018	(1.7)	0.0059	0.008	(0.8)	0.0025	0.006	(0.6)	0.0012	0.099	(8.7)	0.0372
2.95<ρ<3.3	96.51	89.21	0.013	(1.3)	0.0039	0.008	(0.7)	0.0022	0.007	(0.7)	0.0016	0.083	(7.4)	0.0323
2.95<ρ<3.3 magn.	95.27	66.00	0.016	(1.5)	0.0053	0.010	(0.9)	0.0037	0.009	(0.9)	0.0019	0.131	(8.7)	0.0505
2.58<ρ<2.95	95.36	75.46	0.228	(21.8)	0.0768	0.007	(0.7)	0.0022	0.010	(1.0)	0.0020	1.271	(95.9)	0.3636
ρ < 2.58	34.77	25.15	---	---	0.0040	0.012	(0.4)	0.0038	0.021	(0.7)	0.0043	---	---	---
Opx	68.71	65.39	---	---	0.0021	0.007	(0.5)	0.0020	0.004	(0.3)	0.0007	---	---	---
Breccia	34.10	28.72	---	---	0.0083	0.025	(0.9)	0.0072	---	---	0.0017	---	---	---
Whole Rock	100.01	78.09	1.068	(107)	0.3497	0.008	(0.8)	0.0020	0.008	(0.8)	0.0017	0.561	(43.8)	0.2027
Set C : Unleached samples														
Plagioclase (a)	40.74											1.466	(59.7)	0.4546
Olivine (a)	17.29											0.274	(4.7)	0.0929
Olivine (b)	22.17											0.391	(8.7)	0.1315
Pigeonite (b)	21.68											0.141	(3.1)	0.0535
Whole Rock	35.16											0.639	(22.5)	0.2240

Pb-Pb and U-Pb ages (4496 ± 80 Ma and 4082 ± 210 Ma, respectively, for group 3 analyses; 4557 ± 45 Ma and 4480 ± 160 Ma, respectively, for group 4 analyses; BROUXEL and TATSUMOTO, 1990).

The U-Th-Pb data obtained on the five separates of set B (washes, leaches, and residues) are listed in Table 1. It can be seen that very small amounts of U, Th, and Pb were removed by the water and ethanol washing. The very dilute HBr leaching removed greater amounts of Pb, the composition of which is similar to those of the water and ethanol washes (Fig. 2). All washes and leaches have Pb isotopic compositions close to the blank isotopic composition, suggesting that most terrestrial Pb was removed by the leaching process. All the residues plot on a 4553 ± 35 Ma isochron (Fig. 2), except for the troilite which plots below the 4553 Ma isochron. Its isotopic composition is very close to that of the blank. Its very low Pb concentration level (42 ppb) compares well to some troilite grains analyzed in chondrites (UNRUH, 1982) rather than to those found in iron meteorites (TATSUMOTO et al., 1973). If corrected with the measured Pb blank, it plots on a 4569 Ma isochron together with the Cañon Diablo Troilite. If an increased Pb blank correction is used (0.3 ng), the troilite plots with the other points on the 4553 Ma isochron. However, because troilite is known to be dissolved easily even in very dilute acid, the troilite leaching was limited to one minute in an ultrasonic bath while the other samples were leached for five minutes. It is possible, therefore, that this short leaching was not able to remove all the contamination.

The U-Pb data are plotted in Fig. 3 on the modified concordia diagram of TERA and WASSERBURG (1972). The data are corrected using Cañon Diablo Troilite Pb (TATSUMOTO et al., 1973) as the assumed initial Pb isotopic composition. The washes and leaches plot very close to the blank isotopic composition. All the residues plot to the left of the concordia curve, indicating an excess of radiogenic Pb. They define a chord intersecting concordia at 4549 ± 64 Ma and 590 ± 330

Table 3 : Rb-Sr isotopic ratios of the Estherville mesosiderite leaches and residues (T= 4542 Ma).

Sample	$^{87}Rb/^{86}Sr$	$^{87}Sr/^{86}Sr$	$^{87}Sr/^{86}Sr_{(T)}$
Set A :			
HBr (0.1N) leaches			
ρ > 3.3	0.01794 ± 0.0035	0.700460 ± 0.000260	0.699265
ρ > 3.3 magn.	0.00979 ± 0.0024	0.699710 ± 0.000190	0.699057
2.95<ρ<3.3	0.02026 ± 0.0032	0.699980 ± 0.000250	0.698630
2.95<ρ<3.3 magn.	0.00135 ± 0.0020	0.699520 ± 0.000180	0.699430
2.58<ρ<2.95	0.00811 ± 0.0020	0.699510 ± 0.000180	0.698970
ρ < 2.58	0.02657 ± 0.0032	0.699800 ± 0.000240	0.698030
Opx	0.04915 ± 0.0042	0.701860 ± 0.000350	0.698586
Breccia	0.03826 ± 0.0036	0.700460 ± 0.000280	0.697911
Whole Rock	0.00770 ± 0.0016	0.699750 ± 0.000150	0.699237
HCl (2N) leaches			
ρ > 3.3	0.00206 ± 0.0020	0.699720 ± 0.000180	0.699582
ρ > 3.3 magn.	0.00208 ± 0.0032	0.699590 ± 0.000220	0.699451
2.95<ρ<3.3	0.00604 ± 0.0032	0.699630 ± 0.000250	0.699227
2.95<ρ<3.3 magn.	0.00517 ± 0.0018	0.699430 ± 0.000170	0.699085
2.58<ρ<2.95	0.00571 ± 0.0009	0.699343 ± 0.000076	0.698962
ρ < 2.58	0.01310 ± 0.0034	0.699435 ± 0.000250	0.698562
Opx	0.00300 ± 0.0036	0.699802 ± 0.000280	0.699602
Breccia	0.01176 ± 0.0026	0.699660 ± 0.000200	0.698876
Whole Rock	0.00323 ± 0.0014	0.699270 ± 0.000130	0.699055
HF (1N) + HNO_3 (2N) leaches			
ρ > 3.3	0.00447 ± 0.0010	0.699550 ± 0.000090	0.699252
ρ > 3.3 magn.	0.00324 ± 0.0012	0.699250 ± 0.000100	0.699034
2.95<ρ<3.3	0.00318 ± 0.0012	0.699280 ± 0.000075	0.699068
2.95<ρ<3.3 magn.	0.00269 ± 0.0009	0.699190 ± 0.000065	0.699011
2.58<ρ<2.95	0.00243 ± 0.0008	0.699220 ± 0.000060	0.699058
ρ < 2.58	0.00477 ± 0.0008	0.699390 ± 0.000070	0.699072
Opx	0.00519 ± 0.0014	0.699510 ± 0.000120	0.699164
Breccia	0.00442 ± 0.0009	0.699520 ± 0.000085	0.699225
Whole Rock	0.00337 ± 0.0008	0.699320 ± 0.000060	0.699095
Residues			
ρ > 3.3	0.02172 ± 0.0012	0.699800 ± 0.000080	0.698353
ρ > 3.3 magn.	0.02646 ± 0.0014	0.699880 ± 0.000130	0.698117
2.95<ρ<3.3	0.03065 ± 0.0007	0.701040 ± 0.000060	0.698998
2.95<ρ<3.3 magn.	0.02801 ± 0.0006	0.700880 ± 0.000050	0.699014
2.58<ρ<2.95	0.01181 ± 0.0004	0.699790 ± 0.000060	0.699003
ρ < 2.58	0.02465 ± 0.0005	0.700640 ± 0.000055	0.698998
Opx	0.05362 ± 0.0018	0.702400 ± 0.000160	0.698827
Breccia	0.04435 ± 0.0010	0.701740 ± 0.000090	0.698785
Whole Rock	0.03799 ± 0.0012	0.701320 ± 0.000100	0.698789
Set C : Unleached samples			
Plagioclase (a)	0.01066 ± 0.0006	0.699710 ± 0.000040	0.699000
Plagioclase (b)	0.01311 ± 0.0004	0.699880 ± 0.000050	0.699007
Pigeonite (a)	0.01601 ± 0.0004	0.700080 ± 0.000060	0.699014
Pigeonite (b)	0.01562 ± 0.0004	0.700050 ± 0.000050	0.699010
Whole Rock	0.01394 ± 0.0007	0.699940 ± 0.000070	0.699011

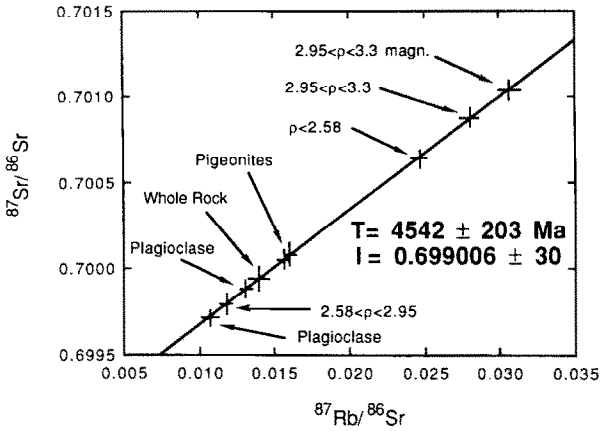

FIG. 4. $^{87}Sr/^{86}Sr$ vs. $^{87}Rb/^{86}Sr$ diagram for nine separates (residues) of the Estherville mesosiderite.

Ma. This upper intercept age is similar to the 4553 Ma Pb-Pb age (Fig. 2). As in the $^{206}Pb/^{204}Pb$ vs. $^{207}Pb/^{204}Pb$ diagram, the troilite plots between the blank isotopic composition and the chord made by the residues.

The Rb-Sr data for sets A and C are given in Tables 2 (concentrations) and 3 (isotopic compositions). Nine residue analyses (from set A, leached, and set C, unleached) define a linear array corresponding to an age of 4542 ± 203 Ma with an initial $^{87}Sr/^{86}Sr = 0.699006 \pm 0.000030$ (Fig. 4). The two plagioclase separates and the $2.58 < \rho < 2.95$ density separate have the lowest $^{87}Sr/^{86}Sr$ and $^{87}Rb/^{86}Sr$ ratios. The $2.58 < \rho < 2.95$ density separate and the plagioclase separate also have similar Sr concentrations (≈60 ppm). The highest Sr concentration was measured in the light density separate (≈80 ppm) which also has a more radiogenic Sr isotopic composition. This separate most likely includes a small percentage of the mesostasis phase described by MURTHY et al. (1977) as a light-density radiogenic phase. The most radiogenic Sr isotopic ratios were measured in the heavy density separates which are enriched in orthopyroxene and pigeonite. Strontium concentrations (2.3 to 8.3 ppm) in these fine-grained heavy density separates are slightly higher than the orthopyroxene separate (1.2 ppm) and are similar to those of the handpicked pigeonites (2.3 and 6.7 ppm). However, the pigeonites have intermediate Sr isotopic composition (Fig. 4).

Our Rb-Sr results are in general agreement with those of MURTHY et al. (1977) with several significant differences. As expected, the pyroxene and the high density fractions are the most radiogenic phases, while plagioclase is the least radiogenic phase. The high and intermediate density fractions contain almost identical Sr concentrations to those reported

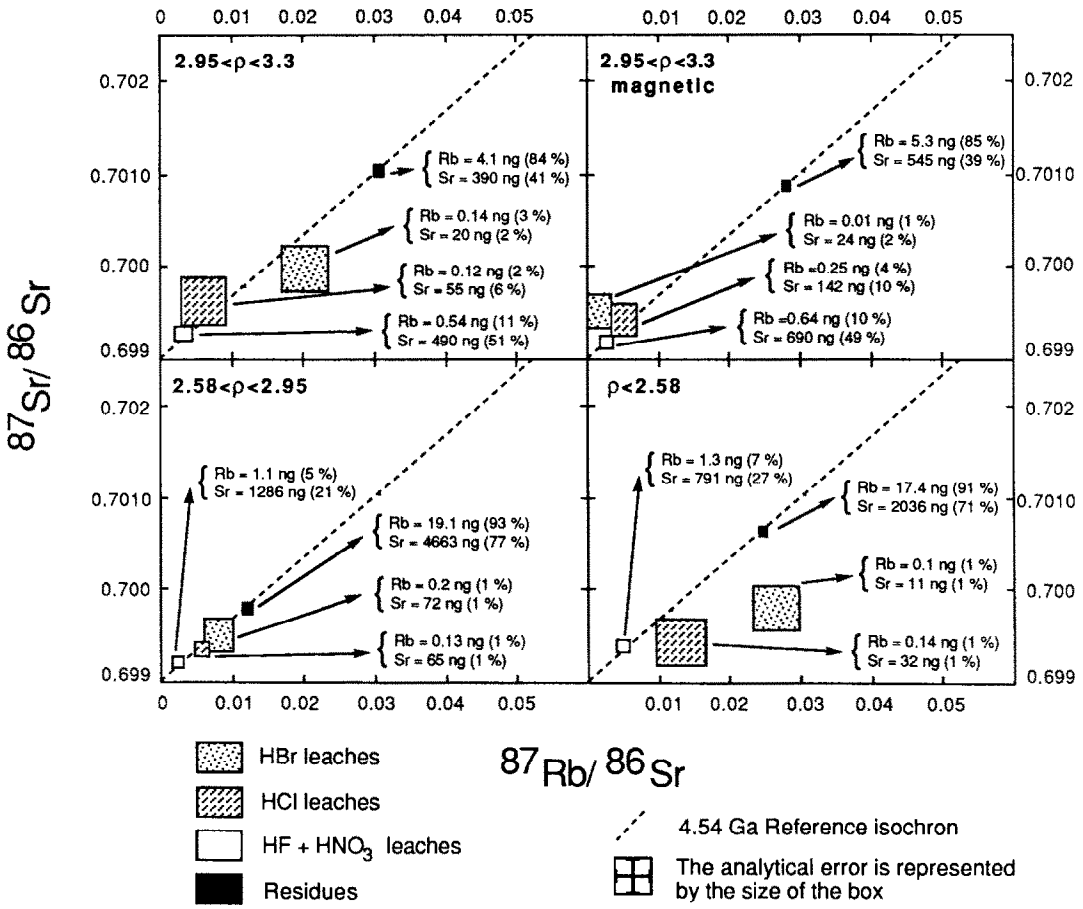

FIG. 5. $^{87}Sr/^{86}Sr$ vs. $^{87}Rb/^{86}Sr$ diagram for the four separates (leaches and residues) of set A which have their HF + HNO_3 leaches and their residues plotting on the 4.54 Ga isochron. The value in parentheses represents the percentage of the total Rb or Sr analyzed in each sample.

by MURTHY et al. (1977), but Sr abundances in the whole-rock and plagioclase separates obtained in this study are much lower. In addition, our data exhibit higher $^{87}Sr/^{86}Sr$ and $^{87}Rb/^{86}Sr$ ratios than those from MURTHY et al. (1977). Some of these differences may be related to our leaching procedure that may have affected the Rb-Sr isotopic system.

All the Rb-Sr data of set A leaches and residues are plotted in Figs. 5 and 6. It can be seen, first, that only small amounts of Rb were leached (the leaches never contain more than 22% of the total Rb) while significant amounts of Sr were leached (usually around 50% of the Sr is measured in the leaches, but up to 75% of the Sr was measured in the whole-rock leaches). Small (negligible?) amounts of Rb and Sr were removed during the HBr (≈1.6 and 1.7%, respectively) and HCl (≈1.5 and 4.4%) leaching. During the HF + HNO_3 treatment, removal of Sr was very important (≈40%) compared to Rb (≈9%). In some cases the amount of Rb analyzed in leaches was very close to the blank level (<0.1 ng). The residues always contain more-radiogenic $^{87}Rb/^{86}Sr$ and $^{87}Sr/^{86}Sr$ ratios compared to the HF + HNO_3 leaches, indicating that our separates contain at least two components: a non-radiogenic component dissolved by the HF + HNO_3 leaching (likely plagioclase), and a more-radiogenic component measured in the residues.

The nine separates of set A reacted differently during the leaching procedure. The four lightest density separates ($2.95 < \rho < 3.3$, $2.95 < \rho < 3.3$ magn., $2.58 < \rho < 2.95$, $\rho < 2.58$), that contained more than 1 μg of Sr before leaching, had their residues and HF + HNO_3 leaches plotting on the 4.54 Ga isochron (Fig. 5). The five other separates show HF + HNO_3 leaches plotting above the 4.54 Ga isochron and residues plotting below this isochron (Fig. 6). Two separates

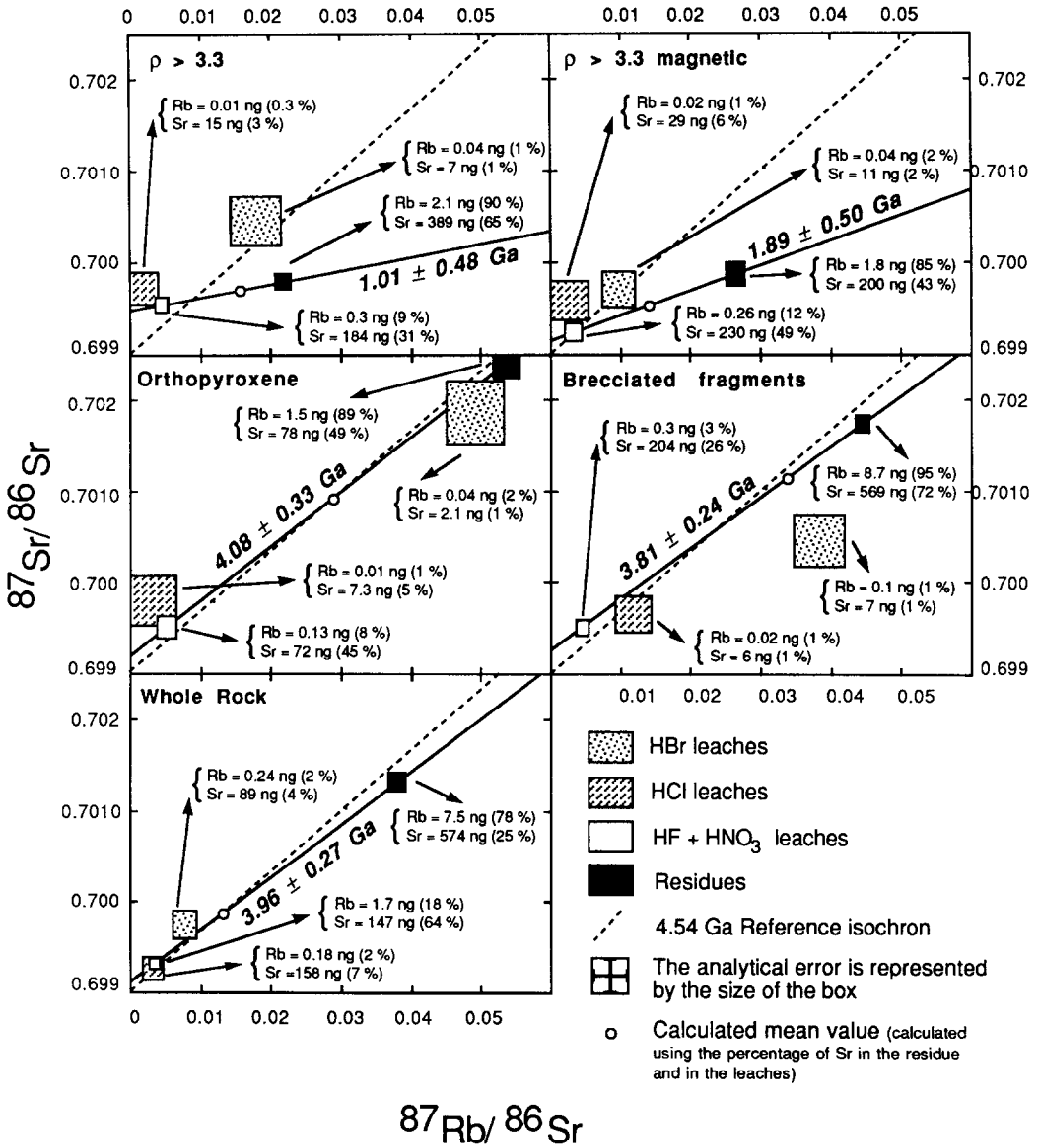

FIG. 6. $^{87}Sr/^{86}Sr$ vs. $^{87}Rb/^{86}Sr$ diagram for the five separates (leaches and residues) of set A which don't have their HF + HNO_3 leaches and residues plotting on the 4.54 Ga isochron. The value in parentheses represents the percentage of the total Rb or Sr analyzed in each sample.

(orthopyroxene and whole-rock) have their calculated mean value (calculated using the percentage of Sr in the residue and in the leaches) plotting on the isochron. The slope of the line joining the residues and the HF + HNO_3 leaches is close to 4.0 Ga (4.08 ± 0.33 Ga and 3.96 ± 0.27 Ga, Fig. 6). The calculated mean value of the brecciated fragments does not plot on the 4.54 Ga isochron, but the slope of the line joining the residue and the HF + HNO_3 leach is also close to 4.0 Ga (3.81 ± 0.24 Ga, Fig. 6). The slope of the line joining the two heavy density fractions residues and HF + HNO_3 leaches give very young ages (1.01 ± 0.48 Ga and 1.89 ± 0.50 Ga; Fig. 6). Their calculated mean values do not plot on the 4.54 Ga isochron.

The Sm-Nd data for sets A and C are given in Tables 2 (concentrations) and 4 (isotopic compositions). Eleven points (from set A, leached, and set C, unleached) define a linear array corresponding to an age of 4533 ± 94 Ma with an initial $^{143}Nd/^{144}Nd$ = 0.506807 ± 0.000020 (ϵ_{Nd} at 4.53 Ga = +1.8 ± 2.0) (Fig. 7).

The $2.58 < \rho < 2.95$ density separate, likely enriched in plagioclase, presents the lowest $^{143}Nd/^{144}Nd$ and $^{147}Sm/^{144}Nd$ ratios. Our plagioclase separate presents a similar Nd concentration (≈1.4 ppm), but higher $^{143}Nd/^{144}Nd$ and $^{147}Sm/^{144}Nd$ ratios. The two olivine separates exhibit almost flat REE patterns ($^{147}Sm/^{144}Nd \approx 0.20$) and very low Nd concentration (≈0.3 ppm). The highest $^{143}Nd/^{144}Nd$ and $^{147}Sm/^{144}Nd$ ratios were measured in the high density separates, likely enriched in orthopyroxene, which present the lowest Nd concentration (0.08 to 0.1 ppm). The pigeonite presents a slightly higher Nd concentration (≈0.14 ppm) compared to the orthopyroxene, but similar $^{143}Nd/^{144}Nd$ and $^{147}Sm/^{144}Nd$ ratios.

In contrast with the Rb-Sr isotopic system, our leaching procedure had very little effect on the Sm-Nd isotopes. Small amounts of REEs were leached, and, more importantly, Sm and Nd apparently did not fractionate during the leaching procedure (Table 2). The HBr leaches contain high, but similar, amounts of Sm and Nd (≈9.9 and 8.8% of the total, respectively), while very small amounts were measured in the HCl (≈4.2 and 3.5%) and HF + HNO_3 (≈2.6 and 2.6%) leaches. In these leaches, the amount of Nd measured was always extremely low (<1 ng in the HCl and HF + HNO_3 leaches; Table 2).

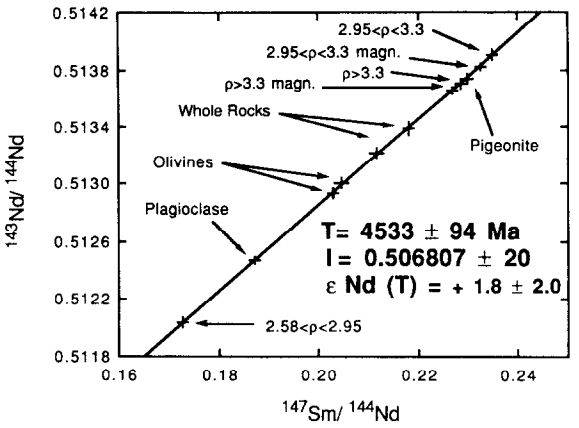

FIG. 7. $^{143}Nd/^{144}N$ vs. $^{147}Sm/^{144}Nd$ diagram for 11 separates (residues) of the Estherville mesosiderite.

DISCUSSION

Pb-Pb and U-Pb Ages

The Pb-Pb and U-Pb ages obtained on set B separates (4553 ± 35 Ma and 4549 ± 64 Ma, respectively) are similar to the Pb-Pb and U-Pb ages of set A group 1 (4556 ± 35 Ma and 4571 ± 18 Ma; BROUXEL and TATSUMOTO, 1990). They confirm that at least part of the mesosiderite silicate fraction was formed early in solar system history (4555 ± 35 Ma and 4560 ± 31 Ma, mean values for the Pb-Pb and U-Pb ages, respectively). This 4.56 Ga age may be compared to some eucrite ages (TATSUMOTO et al., 1973; ALLEGRÈ et al., 1975;

Table 4 : Sm-Nd isotopic ratios of the Estherville mesosiderite leaches and residues (T = 4533 Ma).

Sample	$^{147}Sm/^{144}Nd$	$^{143}Nd/^{144}Nd$	$^{143}Nd/^{144}Nd_{(T)}$	$\epsilon Nd_{(T)}$
Set A :				
HBr (0.1N) leaches				
ρ > 3.3	0.19433 ± 0.00331	0.512732 ± 0.000193	0.506884	3.26
ρ > 3.3 mag	0.19928 ± 0.00205	0.512840 ± 0.000128	0.506843	2.45
2.95<ρ<3.3	0.18199 ± 0.00151	0.512327 ± 0.000146	0.506850	2.59
2.95<ρ<3.3 mag	0.19848 ± 0.00196	0.512730 ± 0.000214	0.506757	0.75
2.58<ρ<2.95	0.20315 ± 0.00091	0.512908 ± 0.000021	0.506795	1.49
Whole Rock	0.19771 ± 0.00081	0.512743 ± 0.000810	0.506793	1.47
Residues				
ρ > 3.3	0.22861 ± 0.00116	0.513684 ± 0.000028	0.506805	1.69
ρ > 3.3 mag	0.22689 ± 0.00100	0.513635 ± 0.000022	0.506807	1.74
2.95<ρ<3.3	0.23484 ± 0.00096	0.513874 ± 0.000035	0.506807	1.74
2.95<ρ<3.3 mag	0.23243 ± 0.00096	0.513800 ± 0.000023	0.506806	1.71
2.58<ρ<2.95	0.17270 ± 0.00102	0.511999 ± 0.000031	0.506802	1.64
Whole Rock	0.21822 ± 0.00103	0.513367 ± 0.000039	0.506800	1.60
Set C : Unleached Samples				
Plagioclase (a)	0.18726 ± 0.00101	0.512443 ± 0.000020	0.506808	1.75
Olivine (a)	0.20471 ± 0.00113	0.512977 ± 0.000032	0.506817	1.93
Olivine (b)	0.20309 ± 0.00103	0.512911 ± 0.000029	0.506800	1.59
Pigeonite (b)	0.22980 ± 0.00102	0.513717 ± 0.000026	0.506802	1.63
Whole Rock	0.21178 ± 0.00113	0.513191 ± 0.000032	0.506818	1.95

CHEN and WASSERBURG, 1985) with which mesosiderites exhibit petrological similarities (DUKE and SILVER, 1967; POWELL, 1971).

Younger ages were obtained for the set A group 2 analyses, with Pb-Pb and U-Pb ages around 4.43 Ga (4422 ± 50 Ma and 4437 ± 11 Ma, respectively; BROUXEL and TATSUMOTO, 1990). These younger ages were obtained on some residues (orthopyroxene, brecciated fragments, $\rho > 3.3$) and leaches. Although terrestrial contamination cannot be completely excluded, we consider this a very unlikely possibility. Samples were repeatedly washed, prior to the HBr leaching, with acetic acid in order to eliminate any iron-coating, water, and alcohol, with acetone after heavy liquid treatments, and with alcohol at the magnetic separation stages. Moreover, the radiogenic nature of the Pb in some leaches ($^{206}Pb/^{204}Pb$ up to 30) suggests that the remaining terrestrial contamination was negligible, if there was any at all. In a TERA and WASSERBURG (1972) modified concordia diagram, the data points plot on an almost horizontal concordia. Therefore, U-Pb fractionation will only displace the points on the same concordia without modifying the resulting age. If we suppose that these ages were not affected by terrestrial contamination, a young Pb component would exist in some mineral phases, some interstitial phases (mesostasis phase, brecciated polycrystalline fragments), or coating of the grains. Therefore, the various minerals (pyroxene, plagioclase, olivine) and lithic (cumulate eucrite, anorthosite, dunite) clasts observed in Estherville (FLORAN, 1978) may have different ages. These younger ages, ranging between 4.42 and 4.44 Ga, compare very well with cumulate eucrites ages (4.41 to 4.46 Ga; LUGMAIR et al., 1977; JACOBSEN and WASSERBURG, 1984; TERA et al., 1987, 1989). The generation of chronological heterogeneity through multiple meteoritic impact events is compatible with previous interpretations of mesosiderites being affected by several generations of brecciation (WASSON and RUBIN, 1985).

Analyses from groups 3 and 4 gave an intermediate Pb-Pb age (4506 ± 75 Ma; BROUXEL and TATSUMOTO, 1990). They were obtained, however, only for the HCl and HF + 9696HNO_3 leaches. In the TERA and WASSERBURG (1972) modified concordia diagram, they present variable $^{207}Pb/^{206}Pb$ initial isotopic ratios, and therefore an U-Pb fractionation during our leaching process affected the $^{238}U/^{206}Pb$ isotopic ratios and, of course, the resulting ages.

The fact that iron plots on the 4553 Ma isochron with the silicate mineral separates indicates that the metal fraction of the Estherville mesosiderite was formed early in solar system history and was likely to have mixed very early with the silicates. This is in agreement with petrological observations indicating that the metal-silicate mixing could have occurred no later than 4.4 Ga ago (BOGARD et al., 1990). It also suggests that iron does not necessarily come from outside the parent body.

Rb-Sr Ages

The Rb-Sr age obtained on nine separates is also close to 4.55 Ga, albeit with a large uncertainty (4542 ± 203 Ma). The age and error reported here are similar to those obtained by MURTHY et al. (1977) on the Estherville mesosiderite if the mesostasis phase is excluded (4.53 ± 0.26 Ga). The initial $^{87}Sr/^{86}Sr$ ratios are also similar (0.699057 ± 0.000030; MURTHY et al., 1977—the machine bias was adjusted using E&A standard run—and 0.699006 ± 0.000030, this study). The large errors obtained on these ages are likely related to the small spread of the $^{87}Rb/^{86}Sr$ and $^{87}Sr/^{86}Sr$ ratios, but may also be related to some sample heterogeneity and/or to some later disturbances. MURTHY et al. (1978) obtained a 4.24 ± 0.03 Ga Rb-Sr age with an initial $^{87}Sr/^{86}Sr$ ratio = 0.699040 ± 20 for Estherville. This age is controlled largely by the mesostasis separate which contains a very radiogenic phase with a high $^{87}Sr/^{86}Sr$ ratio (0.713). Such high Rb/Sr mesostasis phases have been shown to be very sensitive to perturbations (ALLEGRÈ et al., 1975), and it is possible that this 4.24 Ga Rb-Sr age was partially reset by a later metamorphic event.

Additional information regarding a later metamorphic event may be obtained from the leaching results. This leaching procedure was designed to eliminate Pb terrestrial contamination in order to obtain precise Pb-Pb and U-Pb ages, but, in contrast to most studies, we have analyzed those same leaches for Rb-Sr and Sm-Nd isotopes.

Most of the Rb and Sr was found in the HF + HNO_3 leaches and in the residues. The residues were always more radiogenic, suggesting the presence of at least two components in our density separates (Figs. 5 and 6). It can be seen in Fig. 6 that in five cases the HF + HNO_3 leaches and the residues did not plot on the 4.54 Ga isochron, indicating some disturbance of the Rb-Sr isotopic system.

A differential leaching of Rb and Sr during our procedure may explain some of the observed variations: a preferential removal of Sr during the HF + HNO_3 leaching will displace the point toward lower Rb/Sr ratios, while the residue will be moved toward higher Rb/Sr ratios. This would suggest, first, that only some separates have been affected differently by the leaching procedure and, second, that Sr is more easily leached than Rb or that all the leachable Rb was already removed. Moreover, the preferential leaching hypothesis implies that the calculated mean value should always be on the 4.54 Ga isochron which is not true in three cases ($\rho > 3.3$, $\rho > 3.3$ magn., and brecciated fragments; Fig. 6).

An alternative explanation is that the Rb-Sr isotopic system may have been disturbed by a later metamorphic event. When affected by a metamorphic event (around 4.0 Ga) which completely resets the Rb-Sr clock, the whole-rock (calculated mean value) and its two components (HF + HNO_3 leach and residue) will plot on a 4.0 Ga isochron. In the case of a closed system, the whole-rock should also plot on the 4.54 Ga (orthopyroxene and whole-rock). If the system was not closed, or if the resetting was only partial, or in the case of isotopic heterogeneity at 4.54 Ga, the whole-rock (calculated mean value) will not plot on the 4.54 Ga isochron (brecciated fragments). The age of this metamorphic event is not precisely constrained by the Rb-Sr data (3920 ± 150 Ma, excluding two high density fractions; Figs. 6 and 8), and it may be the same as the one recorded by the Ar-Ar isotopes around 3.5–3.7 Ga (BOGARD et al., 1990). A partial resetting of the Rb-Sr isotopic system will yield ages intermediate between 4.56 and 3.5 Ga.

However, neither of these two models are capable of explaining why the two high density fractions show very young Rb-Sr ages between their leaches and residues. A younger

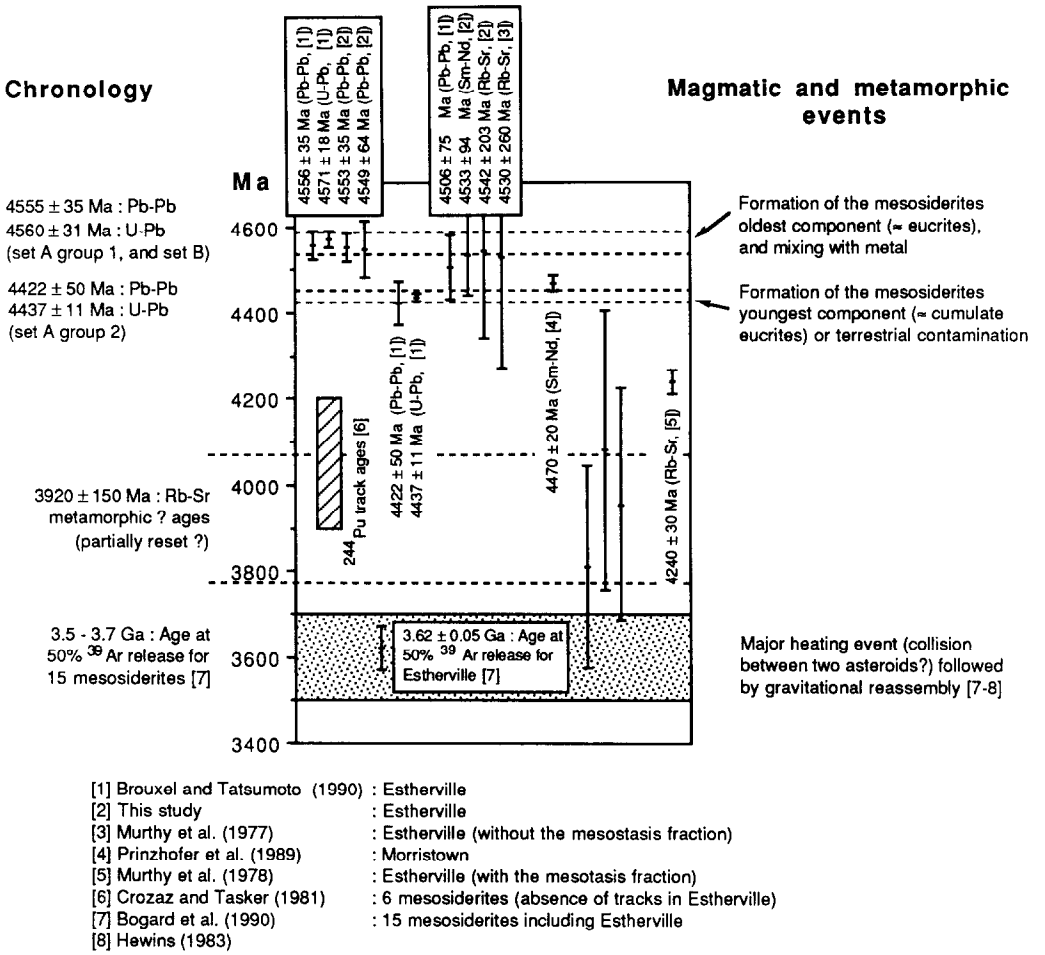

[1] Brouxel and Tatsumoto (1990) : Estherville
[2] This study : Estherville
[3] Murthy et al. (1977) : Estherville (without the mesostasis fraction)
[4] Prinzhofer et al. (1989) : Morristown
[5] Murthy et al. (1978) : Estherville (with the mesotasis fraction)
[6] Crozaz and Tasker (1981) : 6 mesosiderites (absence of tracks in Estherville)
[7] Bogard et al. (1990) : 15 mesosiderites including Estherville
[8] Hewins (1983)

FIG. 8. Summary of the ages obtained on Estherville and some other mesosiderites.

metamorphic event is necessary to explain these younger ages. The later model involving partial resetting of the Rb-Sr system also suggests that the different components of the Estherville mesosiderite reacted differently to the metamorphic event.

Sm-Nd Age

The Sm-Nd isotopic data also do not allow us to determine precisely the age of formation of the Estherville mesosiderite. However, despite its rather large error, the Sm-Nd age of 4533 ± 94 Ma is close to the Pb-Pb and U-Pb age of 4.56 Ga. Like the Rb-Sr isotopic system, the error associated with the Sm-Nd age may be related to the small variations in $^{147}Sm/^{144}Nd$ ratios within the suite, to some sample heterogeneity, or to some metamorphic event that may have slightly disturbed the Sm-Nd isotopic system.

Estherville has a positive ϵ_{Nd} value (+1.8) at 4.53 Ga, but within 2σ error (±2.0) equal to zero. It is, therefore, impossible to define whether Estherville was derived from a chondritic reservoir or a non-chondritic reservoir depleted by previous melting events. Remelting of cumulate gabbro-type rocks has been suggested for other mesosiderites by MITTLEFEHLDT (1990) because of their very LREE-depleted patterns. Our data, at least, do not conflict with this suggestion, but they do not support a complete remelting. Indeed, in that case, no 4.56 Ga Pb-Pb or U-Pb ages would have been obtained.

The fact that our Sm-Nd and Rb-Sr ages present large errors may be therefore related to the mixing between a young and an old component.

CONCLUSION: ORIGIN OF MESOSIDERITES

Despite an increasing number of petrological and geochemical data published on mesosiderites, their origin is unclear. However, integration of ages obtained in this study along with previous age and petrological information published on mesosiderites make it possible to propose a model for their origin.

The Pb-Pb (4555 ± 35 Ma) and U-Pb (4560 ± 31 Ma) ages (Fig. 8) indicate that at least a part of the Estherville silicate fraction was formed early in solar system history. Therefore, mesosiderites exhibit not only petrological but also geochronological similarities with eucrites. Iron, which plots on the same isochron as two silicate separates (4553 ± 35 Ma), probably was also formed, and likely mixed, early in solar system history. This is consistent with the hypothesis that during the magmatic stage, iron was reduced, likely a consequence of metal mixing (AGOSTO et al., 1980; MITTLEFEHLDT et al., 1986b; MITTLEFEHLDT, 1990).

Younger Pb-Pb and U-Pb ages have also been obtained (≈4.43 Ga). These ages are similar to those obtained for cumulate eucrites. They confirm the heterogeneity of the Es-

therville mesosiderite, that is in agreement with the several generations of meteoritic impacts described in mesosiderites by WASSON and RUBIN (1985).

The Sm-Nd and Rb-Sr ages obtained for Estherville are, within error, similar to the 4.56 Ga Pb-Pb ages. These ages, showing large errors, may represent a mixing between the 4.56 and 4.43 Ga endmembers (Fig. 8).

A "rapid cooling" of the mesosiderite parent body would be necessary to explain the presence of ^{244}Pu fission tracks excess in six mesosiderites at ages ranging between 3.9 and 4.2 Ga (CROZAZ and TASKER, 1981). This means that mesosiderites had attained temperatures of less than 100°C by $\approx$4.0 Ga. Such fast cooling is not consistent with the slow cooling rates measured on mesosiderite metals (POWELL, 1969; SAIKUMAR and GOLDSTEIN, 1988; BOGARD et al., 1990). However, it is possible that a thermal event around 3.5–3.7 Ga reset the Ar-Ar ages and the metal cooling textures (BOGARD et al., 1990). A collision between two asteroids followed by gravitational reassembly (HEWINS, 1983; WASSON and RUBIN, 1985) may have been able to produce such a situation.

Acknowledgments—We thank V. R. Murthy for providing the sample. J. B. Paces and D. M. Unruh made helpful reviews of the first draft. Critical comments by L. Nyquist, N. Nakamura, and S. Galer are appreciated. We would like to thank B. D. Marshall and J. Whelan for mineral identification assistance, and W. R. Premo for improving our "franco-japonais" English. This study was supported by NASA Interagency Transfer order T-783-H.

Editorial handling: H. Palme

REFERENCES

AGOSTO W. N., HEWINS R. H., and CLARKE R. S., JR. (1980). Allan Hills A77219, the first Antartic mesosiderite. *Proc. 11th Lunar Planet. Sci. Conf.*, 1027–1045.

ALLEGRÈ C. J., BIRCK J. L., FOURCADE S., and SEMET M. (1975) ^{87}Rb-^{87}Sr age of the Juvinas basaltic achondrite and early igneous activity of the solar system. *Science* **197**, 436–438.

BEGEMANN F., WEBER H. W., VILCSEK E., and HINTENBERGER H. (1976) Rare gas and ^{36}Cl in stony-iron meteorites: Cosmogenic elemental production rates, exposures ages, diffusion losses, and thermal histories. *Geochim. Cosmochim. Acta* **40**, 353–368.

BIRCK J. L. (1986) Precision K-Rb-Sr isotopic analysis: Application to Rb-Sr chronology. *Chem. Geol.* **56**, 73–83.

BOGARD D., MITTLEFEHLDT D., and JORDAN J. (1988) ^{39}Ar-^{40}Ar dating of mesosiderites: A case for major parent body disruption less than 4.0 Gy ago? (abstr.). *Lunar Planet. Sci. Conf.* **XIX**, 112–113.

BOGARD D. D., GARRISON D. H., JORDAN J. L., and MITTLEFEHLDT D. (1990) ^{39}Ar-^{40}Ar dating of mesosiderites: Evidence for major parent body disruption < 4.0 Ga ago. *Geochim. Cosmochim. Acta* **54**, 2549–2564.

BROUXEL M. and TATSUMOTO M. (1990) U-Th-Pb systematics of the Estherville mesosiderite. *Proc. 20th Lunar Planet. Sci. Conf.*, 309–319.

CHEN J. H. and WASSERBURG G. J. (1985) U-Th-Pb isotopic studies on Meteorite ALHA 81005 and Ibitira (abstr.). *Lunar Planet. Sci. Conf.* **XVI**, 119–120.

CROZAZ G. and TASKER D. R. (1981) Thermal history of mesosiderites revisited. *Geochim. Cosmochim. Acta* **45**, 2037–2046.

DELANEY J. S. (1983) The formation of mesosiderites, pallasites and other metal-silicate assemblages: Two mechanisms (abstr.). *Meteoritics* **18**, 289–290.

DUKE M. B., and SILVER L. T. (1967) Petrology of eucrites, howardites and mesosiderites. *Geochim. Cosmochim. Acta* **31**, 1637–1665.

FLORAN R. J. (1978) Silicate petrography, classification and origin of the mesosiderites: Review and new observations. *Proc. 9th Lunar Planet. Sci. Conf.*, 1053–1081.

FLORAN R. J., CAULFIELD J. B. D., HARLOW G. E., and PRINZ M. (1978) Impact-melt origin for the Simondium, Pinnaroo, and Hainholz mesosiderites: Implications for impact processes beyond the earth moon system. *Proc. 9th Lunar Planet. Sci. Conf.*, 1083–1114.

GREENBERG R. and CHAPMAN C. C. (1984) Asteroids and meteorites: Origin of stony-iron meteorites at mantle-core boundaries. *Icarus* **57**, 267–279.

HEWINS R. H. (1983) Impact versus internal origins for mesosiderites. *Proc. 14th Lunar Planet. Sci. Conf.*, 257–266.

JACOBSEN S. B. and WASSERBURG G. J. (1984) Sm-Nd isotopic evolution of chondrites and achondrites, II. *Earth Planet. Sci. Lett.* **67**, 137–150.

JAFFEY A. H., FLYNN K. F., GLENDENIN L. E., BENTLEY W. C., and ESSLING A. M. (1971) Precision measurements of half-lives and specific activities of ^{234}U, and ^{238}U. *Phys. Rev.* **4**, 1889–1906.

LEROUX L. J., and GLENDENIN L. E. (1963) Half-life of thorium 232. *Proc. Natl. Mtg. Nucl. Energy*, 83–94.

LUDWIG K. R. (1980) Calculation of uncertainties of U-Pb isotope data. *Earth Planet. Sci. Lett.* **46**, 212–220.

LUDWIG K. R. (1985a) User's manual for ANALYST, a computer program for control of an Isomass 54 thermal-ionization, single-collector mass-spectrometer. *USGS Open-File Rept. 85-513.*

LUDWIG K. R. (1985b) PBDAT200: A computer program for processing raw Pb-U-Th isotope data. *USGS Open-File Rept. 85-547.*

LUDWIG K. R. (1985c) ISOPLOT200: A plotting and regression program for isotope geochemists, for use with HP series 200 computers. *USGS Open-File Rept. 85-513.*

LUGMAIR G. W. and CARLSON R. W. (1978) The Sm-Nd history of KREEP. *Proc. 9th Lunar Planet. Sci. Conf.*, 689–704.

LUGMAIR G. W., SCHEININ N. B., and CARLSON R. W. (1977) Sm-Nd systematics of the Serra de Mage eucrite. *Meteoritics* **12**, 300–301.

MEGRUE G. H. (1966) Rare gas chronology of calcium-rich achondrites. *J. Geophys. Res.* **71**, 4021–4027.

MITTLEFEHLDT D. W. (1990) Petrogenesis of mesosiderites. I: origin of mafic lithologies and comparison with basaltic achondrites. *Geochim. Cosmochim. Acta* **54**, 1165–1173.

MITTLEFEHLDT D. W., BANSAL B. M., SHIH C. Y., WIESMANN H., and NYQUIST L. E. (1986a) Petrology, chronology and chemistry of basaltic clasts from mesosiderites (abstr.). *Lunar Planet. Sci.* **XVII**, 553–554.

MITTLEFEHLDT D. W., NYQUIST L. E., BANSAL B. M., SHIH C. Y., and WIESMANN H. (1986b) Petrology of type 1A mesosiderites silicates (abstr.). *Meteoritics* **21**, 460.

MURTHY V. R., COSCIO M. R., and SABELIN T. (1977) Rb-Sr internal isochron and the initial ^{87}Sr/^{86}Sr for the Estherville mesosiderite. *Proc. 8th Lunar Sci. Conf.*, 117–186.

MURTHY V. R., ALEXANDER E. C., JR., and SAITO K. (1978) Rb-Sr and ^{40}Ar-^{39}Ar systematics of the Estherville mesosiderite (abstr.). *Lunar Planet. Sci.* **XIV**, 781–783.

NAKAMURA N., TATSUMOTO M., NUNES P. D., UNRUH D. M., SCHWAB A. P., and WILDEMAN T. R. (1976) 4.4 B.Y.-old clast in Boulder 7, Apollo 17: A comprehensive chronological study by U-Pb, Rb-Sr and Sm-Nd methods. *Proc. 7th Lunar Planet. Sci. Conf.*, 2309–2333.

POWELL B. N. (1969) Petrology and chemistry of mesosiderites—I. Textures and composition of nickel-iron. *Geochim. Cosmochim. Acta* **33**, 789–810.

POWELL B. N. (1971) Petrology and chemistry of mesosiderites—II. Silicate textures and compositions and metal-silicate relationships. *Geochim. Cosmochim. Acta* **35**, 5–34.

PREMO W. R., TATSUMOTO M., and WANG J. W. (1989) Pb isotopes in anorthositic breccias 67075 and 62237: A search for primitive lunar lead. *Proc. 19th Lunar Planet. Sci. Conf.*, 61–71.

PRINZHOFER A., PAPANASTASSIOU D. A., and WASSERBURG G. J. (1989) The presence of ^{146}Sm in the early solar system and implications for its nucleosynthesis. *Astrophys. J.* **344**, 81–84.

PRIOR G. T. (1920) The classification of meteorites. *Mineral. Mag.* **19,** 51–63.

SAIKUMAR V. and GOLDSTEIN J. I. (1988) An evaluation of the methods to determine the cooling rates of iron meteorites. *Geochim. Cosmochim. Acta* **52,** 715–726.

TATSUMOTO M., KNIGHT R. J., and ALLEGRÈ C. J. (1973) Time differences in the formation of meteorites as determined by the $^{207}Pb/^{206}Pb$. *Science* **180,** 1279–1283.

TATSUMOTO M., HEGNER E., and UNRUH D. M. (1987) Origin of the West Mauai volcanics inferred from Pb, Sr, and Nd isotopes and a multi-component model for oceanic basalts. *USGS Prof. Pap.* **1350,** 723–744.

TERA F. and WASSERBURG G. J. (1972) U-Th-Pb systematics in three Apollo 14 basalts and the problem of initial Pb in lunar rocks. *Earth Planet. Sci. Lett.* **14,** 281–304.

TERA F., CARLSON R. W., and BOCTOR N. Z. (1987) Isotopic and petrologic investigation of the eucrites Cachari, Moore County and Stannern (abstr.). *Lunar Planet. Sci. Conf.* **XVIII,** 1004–1005.

TERA F., CARLSON R. W., and BOCTOR N. Z. (1989) Contrasting Pb-Pb ages of the cumulate and non-cumulate eucrites (abstract). *Lunar Planet. Sci. Conf.* **XX,** 1111–1112.

UNRUH D. M. (1982) The U-Th-Pb age of equilibrated L chondrites and a solution to the excess radiogenic Pb problem in chondrites. *Earth Planet. Sci. Lett.* **58,** 75–94.

UNRUH D. M., NAKAMURA N., and TATSUMOTO M. (1977) History of the Pasamonte achondrite: Relative susceptibility of the Sm-Nd, Rb-Sr, and U-Pb systems to metamorphic events. *Earth Planet. Sci. Lett.* **37,** 1–12.

UNRUH D. M., STILLE P., PATCHETT P. J., and TATSUMOTO M. (1984) Lu-Hf and Sm-Nd evolution in Lunar Mare Basalts. *Proc. 14th Lunar Planet. Sci. Conf.,* 459–477.

WASSERBURG G. J., JACOBSEN S. B., DEPAOLO D. J., MCCULLOCH M. T., and WEN T. (1981) Precise determination of Sm/Nd ratios, Sm and Nd isotopic abundances in standard solutions. *Geochim. Cosmochim. Acta* **45,** 2311–2323.

WASSON J. T. and RUBIN A. E. (1985) Formation of mesosiderites by low velocity impacts as a natural consequence of planet formation. *Nature* **318,** 168–170.

YORK D. K. (1969) Least squares fitting of a straight line with correlated errors. *Earth Planet. Sci. Lett.* **5,** 320–324.